

# Dynamic experimental analysis of a LiBr/H<sub>2</sub>O single effect absorption chiller with nominal capacity of 35 kW of cooling

Alvaro Antonio Ochoa Villa<sup>1,2\*</sup>, José Carlos Charamba Dutra<sup>2</sup>, Jorge Recarte Henríquez Guerrero<sup>2</sup>, Carlos Antonio Cabral dos Santos<sup>2,3</sup> and José Ângelo Peixoto da Costa<sup>1,2</sup>

<sup>1</sup>Instituto Federal de Tecnologia de Pernambuco, Avenida Professor Luiz Freire, 500, 50740-540, Recife, Pernambuco, Brazil. <sup>2</sup>Universidade Federal de Pernambuco, Avenida Professor Moraes Rego, 1235, 50670-901, Recife, Pernambuco, Brazil. <sup>3</sup>Universidade Federal da Paraíba, João Pessoa, Pernambuco, Brazil. \*Author for correspondence. E-mail: [ochoaalvaro@recife.ifpe.edu.br](mailto:ochoaalvaro@recife.ifpe.edu.br)

**ABSTRACT.** This paper examines the transient performance of a single effect absorption chiller which uses the LiBr/H<sub>2</sub>O pair with a nominal capacity of 35 kW. The goal of this study is to verify the absorption chiller when it is subjected to thermal loads and its capacity to respond transiently as a result of the temperature of the chilled, cold and hot water of the system. An experimental methodology was established in a microgeneration laboratory to simulate the dynamic operating conditions of the system by considering the thermal load (chilled water), the activation source (hot water) and the heat dissipation circuit (cold water). The thermal load was simulated based on using a set of electrical resistors installed in a water heater and on activating the chiller from gas recovered from a 30 kW microturbine and by using a compact heat exchanger where the water is heated and sent in a hot water buffer tank where it was stored. The heat dissipation system of the absorption chiller consists of a pump and a cooling tower. The system responded appropriately to the thermal load imposed and provided coefficient of performance values in the transient regime of 0.55 to 0.70 for the temperature conditions tested.

**Keywords:** energetic behavior; lithium bromide/water solution; thermal load; COP.

Received on February 1, 2017.  
Accepted on September 20, 2017

## Introduction

Absorption systems represent an energy and economical alternative which set out to replace mechanical compression systems in the area of refrigeration and air conditioning. Although an absorption system has a lower COP when compared to a mechanical compression system, it presents a great advantage since it can be driven by thermal rejects. This is linked to the use of energy cogeneration, and, therefore, associated to a decrease in the direct consumption of electricity in addition to which the cost of maintaining absorption systems is low, since they do not have moving parts (Huicochea, Rivera, Gutiérrez, Bruno, & Coronas, 2011; Ochoa, Dutra, Henríquez, & Rohatgi, 2014).

Absorption refrigeration systems have been studied by using analysis of the 1st and 2nd Law of Thermodynamics, considering conditions of permanent regime (Somers et al., 2011; Ochoa et al., 2014) and also, a transient regime (Zinet, Rulliere, & Haberschill, 2012; Evola, Le Pierrès, Boudehenn, & Papillon, 2013; Ochoa, Dutra, Henríquez, & Santos, 2016), the purpose of which is to verify the influence of technical parameters such as; temperature, pressure and flow on the COP of the system.

Another way of analyzing absorption refrigeration systems, under steady state conditions, is to apply the characteristic equation method, which was developed from approximating the behavior of items of absorption refrigeration equipment by making multilinear adjustments and regressions using experimental data and/or the manufacturer's specifications (Puig, López, Bruno, & Coronas, 2010; Gutiérrez-Urueta, Rodríguez, Ziegler, Lecuona, & Rodríguez-Hidalgo, 2012). In this context, the importance of experimental data that allow the real behavior of absorption systems to be verified, as well as of obtaining databases that allow curves and functions of comparison to be adjusted is great, as these data can be applied when validating numerical models (Marc, Sinama, Praene, Lucas, & Castaing-Lasvinottes, 2015), designing control strategies (Seo, Shin, & Chung, 2012), taking advantage of the uses of solar energy as a driven source (Tsoutsos, Aloumpi, Gkouskos, & Karagiorgas, 2010; Venegas et al. 2011; Olivier, Praene, Bastide, & Franck, 2011; Edem, Le Pierrès, & Luo, 2012) and for cogeneration system applications (Popli, Rodgers, & Evely, 2013; Ochoa et al. 2014).

Different experimental and/or real studies have been developed that seek a better understanding of absorption refrigeration systems that use commercial mixtures pairs such as: LiBr/H<sub>2</sub>O and NH<sub>3</sub>/H<sub>2</sub>O (Moya et al., 2011; Ozgoren, Bilgili, & Babayigit, 2012; Ochoa, Dutra, Henríquez, Santos, & Rohatgi, 2017). Izquierdo, Marcos, Palacios, and González (2012) describe a prototype direct-cooled air-cooled double-acting absorption system using the LiBr/H<sub>2</sub>O pair by burning natural gas and evaluate its performance. This prototype was built in Madrid (Izquierdo et al., 2012), with a cooling capacity of 7 kW, the chilled water reaching temperatures of between 7 to 18°C for specific temperatures of the external environment. In the same context, Prasartkaew (2014), presented an analysis of the performance of a rebuilt small absorption refrigeration unit. The study enabled it to be verified that to obtain high COPs, hot water with a temperature of around 85°C in the generator had to be supplied. In the studies by Zamora, Bourouis, Coronas, and Vallès (2014; 2015), an absorption refrigeration prototype using the NH<sub>3</sub>/LiNO<sub>3</sub> pair as working fluid was presented. The novelty of this prototype was the advantage in its thermodynamic properties such as: elimination of the crystallization problem for the operating conditions, and low driven temperatures that can be reached in an integral way from solar energy. The system was built using plate heat exchangers due to the compactness of the system and its being simple to operate, besides which it has a system for dissipating heat into the air (air-heater). The thermal COPs achieved with this prototype were approximately 0.6, which makes the prototype feasible as an alternative to commercial equipment already on the market.

It is noteworthy that there are such a large number of studies that deal with absorption chillers with single, double and even triple effects, but they are limited to the conditions of process stability (Labus, Bruno, & Coronas, 2013; Wang & Wu, 2015). However, on seeking to determine the actual behavior of such equipment when it is subjected to disturbances, whether thermal load and/or energy source, its transient behavior needs to be verified (Monné, Alonso, Palacín, & Serra, 2011; Edem et al., 2012), because, this is what leads to a real understanding of how they operate. Hence, the importance of studies on real operation which enable a more suitable form of control to be found for enhancing the performance of refrigeration absorption systems, as these systems are frequently limited to the conditions imposed by the control system built for their operation.

Therefore, this study was directed at the transient performance of an absorption chiller of 35 kW refrigeration capacity, and its influence on the COP as a result of the dynamic variation of the thermal load to which the system is submitted, considering real operating conditions (hot, cold and chilled water temperatures).

### Material and methods

The experimental analysis was carried out from the tests conducted in the micro-generation laboratory of the Department of Mechanical Engineering of UFPE. The data collected from the absorption chiller were, basically, the temperatures of the hot, cold and chilled water circuits, as well as flow measurements of these circuits. Figure 1a shows an overall scheme of the microgeneration laboratory used in the experimental study, and Figure 1b shows the absorption refrigeration cycle, the target of this study.

The micro-cogeneration process is started by burning a mixture of air and natural gas in the microturbine, which generates electricity. The heat rejected in the combustion gases is reused by transferring it to a compact cross-over heat recovery unit. This energy contained in the flue gases was recovered by heating water, which was stored in the thermo-accumulator (Hot water tank).

This water is sent through a system of pipes and circulation pumps to the absorption chiller where it is activated, and subsequently is used to produce chilled water. This water is pumped to the chilled water storage tank where it is stored. A thermal disturbance was introduced into this thermo-accumulator due to the heat dissipation produced by the electrical resistances installed inside the tank, in order to simulate the real thermal load of an absorption refrigeration system. All the heat removed from the evaporator in the production of chilled water (internal cooling of the equipment) was dissipated through the cold water circuit by using a pump and cooling tower assembly. It is important to point out that producing electric energy was not the objective of this study, but exhaust gases had to be produced so as to heat the water, and supply the energy to drive the absorption chiller.

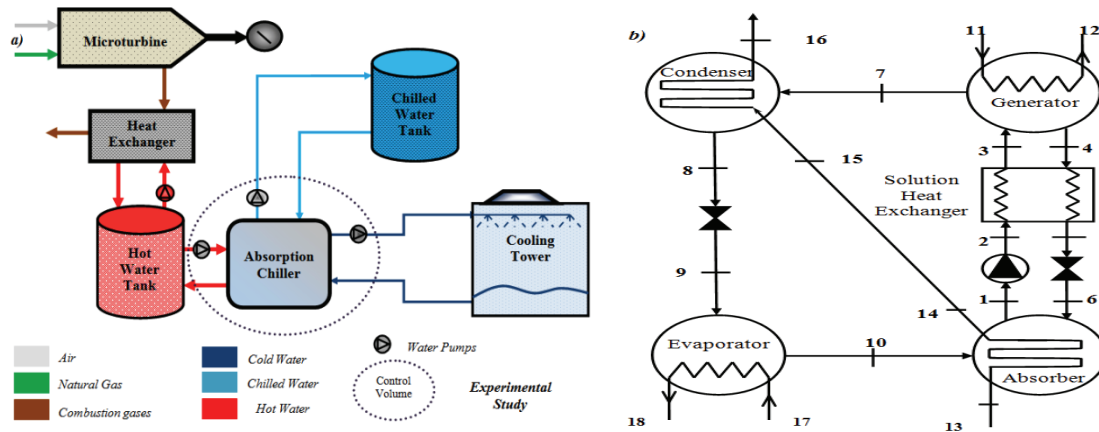


Figure 1. a) Microgeneration system used in the experimental analysis of the absorption refrigeration machine. b) Absorption refrigeration cycle.

### Absorption refrigeration system

A single-effect absorption refrigeration system is a device that works at very low (vacuum) pressure, and consists of four main components, namely an absorber, a generator, a condenser and an evaporator and some auxiliary components, Figure 1b. This equipment has three external circuits (hot, cold and chilled water circuits) and an internal circuit (refrigerant and/or LiBr/H<sub>2</sub>O solution). The internal fluid is responsible for the process of desorption, absorption, condensation and vaporization, points 1-10. The external circuits are distributed by points (11-12) of the hot water, (13-16) cold water, and (points 17-18) chilled water, which are, respectively, responsible for activating the equipment, internal cooling (heat dissipation) and the refrigerator (cooling capacity), respectively. The source of activation of the absorption refrigeration system comes from the hot water circuit heated through the cogeneration system. This hot water circuit (which passes through 11 and 12) exchanges heat with the LiBr/H<sub>2</sub>O solution, heats it and vaporizes it inside the generator. The vapor produced (point 7) passes through the condenser where it exchanges heat with the cold water circuit (15-16), thus condensing it, and this condensate passes through an expansion valve (points 8-9) in which its pressure and temperature are reduced. The condensate is then sent to the evaporator, where the cooling effect occurs by means of heat exchange with the chilled water (17-18), thereby vaporizing the refrigerant (point 10). This low pressure saturated refrigerant vapor enters the absorber where it is mixed with the weak and strong solution (points 1 and 6) by dissipating heat from the cold water (points 13-14). This effect is called absorption. The weak LiBr solution is pumped to the generator (point 1), and the process starts again. The heat exchanger located between the generator and the absorber (points 2-3 and 4-5) improves the coefficient of performance (COP) of the absorption chiller due to the preheating of the solution which returns to the generator through the heat supplied by the strongly concentrated solution which flows from the generator.

### Experimental apparatus

The main items of equipment used in the experimental tests were: a 30 kW Capstone microturbine, a compact heat recuperator, a hot water tank, a 10 TR absorption chiller, a chilled water tank, a cooling tower, and a water pumping system for the water circuits.

### Absorption chiller - 10 RT (LiBr/H<sub>2</sub>O)

The absorption chiller uses the LiBr/H<sub>2</sub>O pair as a working fluid (Figure 2a) and has a 35 kW nominal capacity, the hot and cold water inlet temperatures being 90 and 31°C, respectively, while the outlet temperature of the chilled water is 7°C. The chiller is made operational indirectly, the hot water used for its activation being supplied by the driven system (Figure 2b). The chilled water produced was stored in the hot water tank (Figure 3a) and the cold water circuit of the cooling tower (Figure 3b) was used to dissipate heat.

### Driven source of the absorption chiller

The activation system of the absorption chiller consists of three components: a gas microturbine of 30 kW of electric power, a type of compact heat recovery unit, and a cylindrical hot water tank with an approximate capacity of 800 L. Figure 2b shows the microturbine (right), the heat recuperator (center), and the water storage tank (left), from which hot water is pumped to activate the microturbine.

### Chilled water thermo accumulation system - thermal load

The chilled water storage system, Figure 3a, consists of a set of electrical resistances with a maximum capacity of 35 kW (3 of 10 kW and 1 of 5 kW), which is responsible for simulating the thermal load of the

absorption chiller. This thermo-accumulator is fully instrumented with thermocouples to measure the inlet and outlet temperatures of the chilled water circuit.

#### Dissipation heat systems (pump and cooling tower)

The heat dissipation system of the absorption chiller, Figure 3b, comprises the pump and cooling tower of the induction type with a nominal capacity of 100 kW. This cooling tower is connected to the closed circuit of the cold water of the system through the heat exchangers of the absorber and condenser (series flow) and its function is to dissipate the total heat generated internally in the absorption and condensation processes of the chiller. This system was also fully instrumented with thermocouples to measure the temperatures of the cold water circuit as well as the temperatures of the air introduced to the cooling tower.

#### Instruments and measuring sensors

The measuring instruments used in the tests were type J thermocouples (iron/constantan alloy) for the temperature range (from  $-270$  to  $760^{\circ}\text{C}$  and uncertainties of the order  $\pm 0.75\%$ ), and were placed throughout the hot, cold and chilled water circuits. They are responsible for measuring the temperatures of the system. The thermocouples were strategically installed at the inputs and outputs of the cold, hot and chilled water circuits (Figure 4a) from left to right, for real system measurements. There are other thermocouples installed in the laboratory, but it was not in the interest of this experimental work.

A flow meter, supplied by the manufacturer of the absorption chiller (Yazaki Energy System, 2003), was used to measure and configure the mass flows rate of the cold, hot and chilled water circuits, within the limits established for its operation with accuracy of an order of  $\pm 0.5\%$ . Each input and output of the cold and chilled water circuits has a pressure test valve, Figure 4b. A pressure gauge was used to take the reading of the pressure difference.

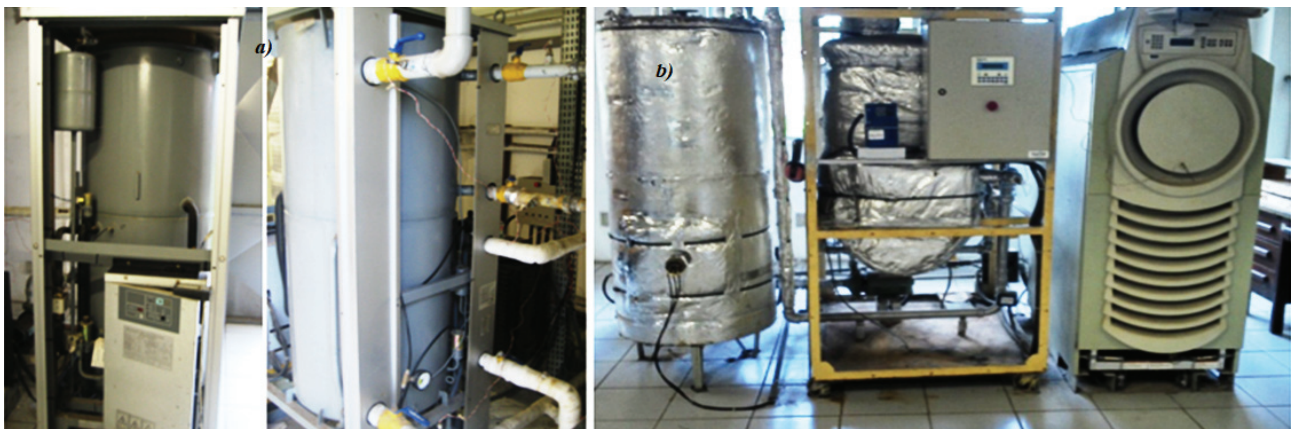


**Figure 2.** a) LiBr/H<sub>2</sub>O Absorption Chiller. b) Power source of the absorption chiller (Hot water tank, recovery heat exchanger and microturbine).



**Figure 3.** a) Electric resistor set and chilled water tank. b) Cooling Tower – Cold water circuit.

**Data acquisition system**

The laboratory has a central monitoring and data storage system. This system allows data to be stored with measurement intervals for each selected time step. The supervisory system was created in the Eclipse Scada commercial software to monitor and control all the functions of the micro-cogeneration laboratory. The supervisor consists of three main circuits; cold, hot water and cold. However, for this specific study, only hot and cold water circuits were used. The experimental data measured were statistically treated (means, uncertainties and errors), with maximum uncertainty values (MUVs), as follows: The input and output hot water circuit with MUVs in the order of 0.11 and 0.13, respectively. The cold water inlet and outlet circuit with MUVs in the order of 0.13 and 0.13° C, respectively. The inlet and outlet chilled water temperature circuit with MUVs in the order of 0.15 and 0.12°C, respectively. The uncertainties of the mass flow, 0.023, 0.033 and 0.018 kg s<sup>-1</sup> of the hot, cold and chilled circuits were 0.023, 0.033 and 0.018 kg s<sup>-1</sup>, respectively.

**Evaluation of the performance of the absorption chiller**

The performance of the absorption chiller was calculated from the temperature measurements of the hot, cold and chilled water circuits, as well as from the mass flow rates. To determine the COP of the chiller ( $COP_{thermal}$ ) it was necessary to calculate the heat of; the generator ( $\dot{Q}_{gen}$ ) the evaporator ( $\dot{Q}_{eva}$ ) and the absorber/condenser system ( $\dot{Q}_{abs/con}$ ) by using First Law of Thermodynamics Equation 1, 2, 3 and 4, expressed as:

$$\dot{Q}_{gen} = \dot{m}_{hot,w} \cdot cp_w \cdot (T_{hot,w,in} - T_{hot,w,out}) \quad (1)$$

$$\dot{Q}_{eva} = \dot{m}_{chilled,w} \cdot cp_w \cdot (T_{chilled,w,in} - T_{chilled,w,out}) \quad (2)$$

$$\dot{Q}_{abs/con} = \dot{m}_{cold,w} \cdot cp_w \cdot (T_{cold,w,out} - T_{cold,w,in}) \quad (3)$$

$$COP_{thermal} = \frac{\dot{Q}_{eva}}{\dot{Q}_{gen}} \quad (4)$$

where:

$cp_w$ , is the specific heat of the water,  $\dot{m}_{hot,w}$ ,  $\dot{m}_{chilled,w}$ ,  $\dot{m}_{cold,w}$  are the mass flow rates of the hot, chilled and cold water,  $T_{hot,w,in}$ ,  $T_{hot,w,out}$ ,  $T_{chilled,w,in}$ ,  $T_{chilled,w,out}$ ,  $T_{cold,w,out}$ ,  $T_{cold,w,in}$ , are inlet and outlet of the hot, chilled and cold temperatures, respectively.



**Figure 4.** a) Temperature measurement point of the external water circuits, used in the microgeneration laboratory (cold, hot and chilled water, respectively). b) Pressure reading socket used to measure the mass flow water rate and pressure difference of the water circuits (Yazaki Energy System, 2003).

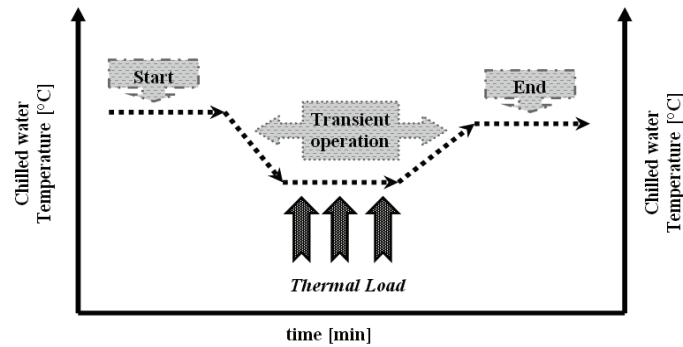


**Figure 5.** Representative scheme of the thermal load procedure used to evaluate the dynamic behavior of the absorption chiller.

### Discussion and results

The dynamic evaluation of the absorption chiller studied (WFC-SC10) was performed considering two typical days of data collection. The difference between each test day falls on the measured flows of the external circuits. On Day 1, the nominal machine operating mass flow rates of the hot, cold and chilled water circuits (2.40, 5.09 and 1.53 kg s<sup>-1</sup>), respectively, were chosen and, on Day 2, the mass flow rate with values of (2.55, 5.09 and 1.8 kg s<sup>-1</sup>) of the hot, cold and chilled circuits, respectively.

#### Day 1

For this test day, the measured flow rates were 2.40, 5.09 and 1.53 kg s<sup>-1</sup>, of hot, cold and chilled water, respectively. The temperature values of the hot, cold and chilled water of the absorption chiller circuits were collected at intervals of 30 seconds. However, to present the results, the values were collected every 10 minutes, since the variations between these different intervals were minimal. Figures 6a and 7b and Figure 7a show the temperature profiles of the hot, cold and chilled water circuits, respectively. Figure 7b shows the heat flow rates of the absorption chiller circuits (generator, evaporator and condenser/absorber).

Figure 6a shows that the hot water temperature values on entering the absorption chiller suffer a sudden drop in energy, due to the under-dimensioning of the thermo-accumulator in the laboratory, which leads to an initial decrease of energy when the system begins the operation, that is, the thermal load of the water is withdrawn.

This phenomenon does not affect the general behavior of the equipment, but it describes the real behavior of the micro-cogeneration system installed at the UFPE laboratory. After the system has been operating for approximately 100 min, it reaches the permanent state, that is, at this moment the entire thermal load of the water contained in the tank (thermo-accumulator) was removed.

Thereafter, the nominal heat load of the absorption chiller is introduced from the connection of the electrical resistances which begin to dissipate heat to the chilled water. This phenomenon can be observed in Figure 6b, where the temperature of the chilled water begins to increase due to the addition of heat. There is an overall increase in temperature of 2°C which lasts for about 100 minutes, after which the system consumes more activation energy (hot water) and the temperature of the hot water tends to drop (by approximately 1.5°C) for a few minutes (Figure 7b) due to the heat system being required to remove the dynamic load introduced.

After this time interval following which the absorption chiller removed the thermal load introduced, the system goes on steady state again, leaving the temperature of the chilled water around 11°C, and the hot water temperature at the inlet and outlet at 87 and 82°C, respectively. All of these temperature variations of the hot and cold water circuits, where heat was supplied to the chiller to remove the required thermal load of the chilled water, leads to heat dissipation for internal cooling, as shown in Figure 7b, which also shows the variation of the cold water circuit responsible for carrying out this process.

It can be seen that the cold water temperature remains almost constant, around 29 and 32°C, throughout the whole process, as this depends both on the capacity of the cooling tower (100 kW), a capacity rated higher than that required by the absorption chiller (88 kW), and also on the conditions of the air temperature and the nominal flow rate maintained throughout the process.

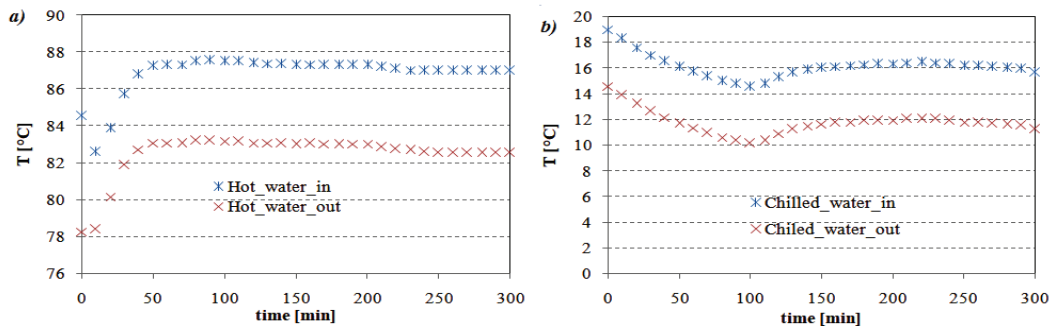


Figure 6. Profile of the temperature in transitory state – day 1. a) Hot Water b) Chilled Water.

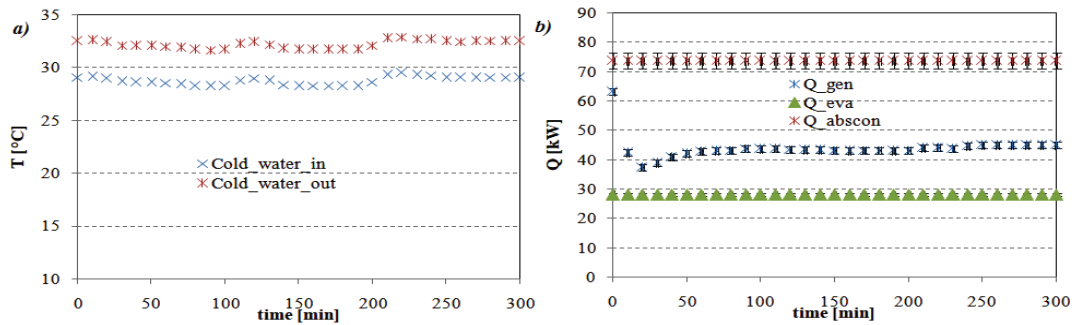


Figure 7. Profile of the temperature in transitory state – day 1. a) cold water b) Heat flows rate.

The temperature differences of the hot, chilled and cold water circuits of the absorption chiller were about 4.5, 4.5 and 3.5 K, respectively. These differences are in agreement with the nominal values shown by the manufacturer of 4, 5.5 and 4 K. It is important to remember that the system was operating out of the nominal conditions, i.e. partial load, and the idea of this study is to show the real behavior of the refrigeration system when subjected to variable loads in time and their influence on the thermal COP.

Figure 7b shows that the heat flow of the cold water circuit (condenser/ absorber) is almost constant, because this circuit is almost unaffected by the applied thermal load, since it depends on the air temperature and its capacity to remove heat, which in this case is greater than that required by the equipment. The value of this dissipation cold water flow was approximately 74 kW. On the other hand, there is significant variation in the hot water circuit (generator) due to the limitations of the hot water tank (lower capacity) and the requirement of more activation energy to remove the heat introduced due to the heat generated by the electrical resistances. The value of hot water flow rate varies between 60 and 40 kW throughout the process, with the absorption chiller being more significant at the beginning of the operation. The heat flow rate of the chilled water circuit (evaporator) (varies hardly ever varies from 31 kW). This is mainly due to the ability of the absorption chiller to withdraw the heat and maintain the temperature conditions, i.e., the temperature difference is almost constant despite the value of the return temperature to the system, whenever it is within the range of the operating system.

### Day 2

For this test day, the hot and cold water flow rates were varied ( $2.55$  and  $1.75 \text{ kg s}^{-1}$ ), respectively, the cold water flow rate remaining at the same value as the nominal. The idea was to verify the behavior of the absorption chiller at partial load situations, that is, outside the rated flows indicated by the manufacturer. Figures 8a and b and Figure 9a show the temperature profiles of the hot, cold and chilled water circuits, respectively. Figure 9b shows the heat flows of the absorption chiller circuits.

To avoid the problem of sizing the hot water tank, which is explained above, this test was carried out at a higher hot water temperature, and thus the temperature drop at the start was much lower. The difference in the temperature of the hot water (input and output) increases, by around 5.3 K, Figure 8a, due to the increase in the mass flow rate in this circuit ( $2.55 \text{ kg s}^{-1}$ ), since the system requires more energy to drive the chiller, when the calculated heat flux rate was around 55 kW.

On the other hand, although the difference in the temperature of the cold water increases (4.1 K), Figure 8b, the heat flow in the evaporator was almost constant ( $\approx 30 \text{ kW}$ ). Once again it can be seen that the temperature of the cold water remains almost constant, around 28 and 32°C, throughout the process, Figure 9a. This phenomenon is similar to what Figure 7a shows happened. Basically, this process depends on the cooling tower having a higher rated capacity, and on the air temperature and nominal flow rate conditions.

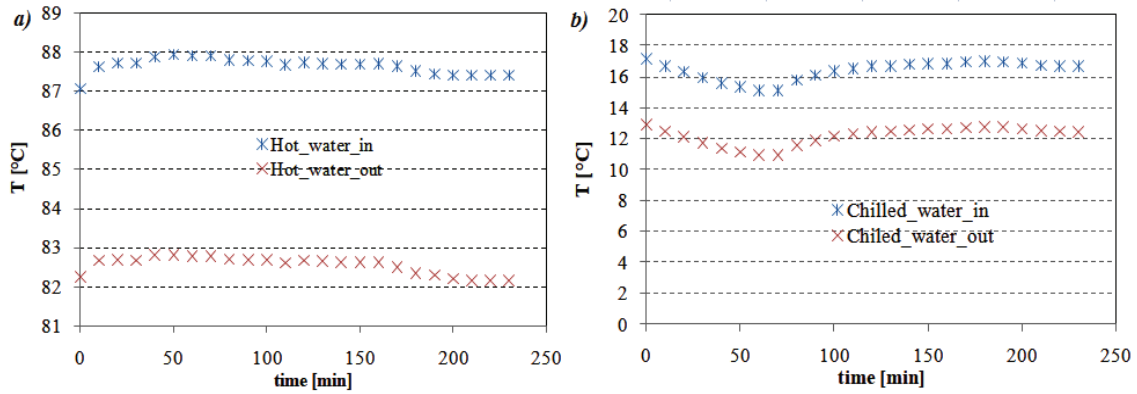


Figure 8. Profile of the temperature in transitory state – day 2. a) Hot Water b) Chilled Water.

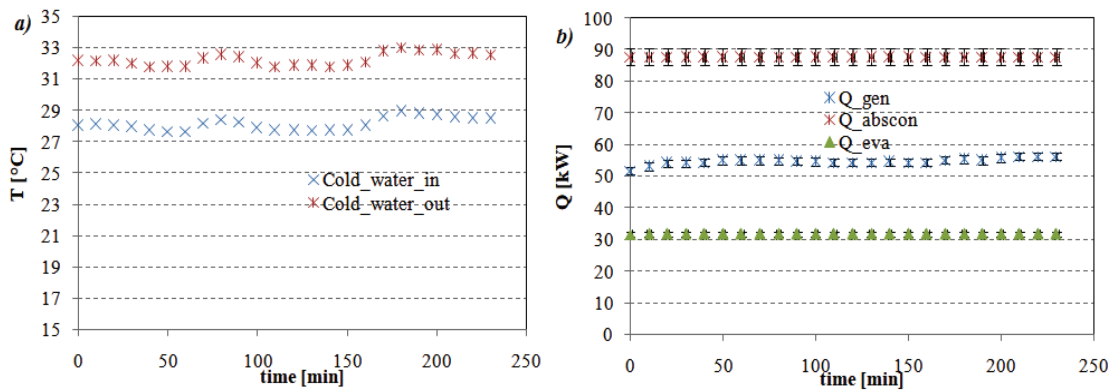


Figure 9. Profile of the temperature in transitory state – day 2. a) cold water b) Heat flows rate.

The variations in the heat flows of the generator and evaporator lead to the slight increase in the dissipation heat flow of the cold water of the chiller, Figure 9b, which had an approximate value of 88 kW, while the difference in temperature between the input and output of this circuit was 4 K. It is important to note that the variations in the flows of the hot and chilled water circuits lead to these having a higher energy effect on the evaporator, as well as to increasingly activating the absorption system. Figures 10a and b show the profiles of the COPs throughout the transient process of the absorption chiller during the days analyzed (1 and 2).

Note that initially the COP of the system is low, since this the moment at which the system tries to overcome its own thermal inertia and also that of the chilled water, which initially was at the ambient temperature of 19°C. The value of the COP ranges from 0.55 to 0.69 for the entire operational range of the test on Day 1. These values are in accordance with the values shown by the manufacturer for nominal conditions. In other words, even when the chiller is operating at partial load, its efficiency may be optimal, since an absorption refrigeration system subjected to sudden thermal loads can be recovered and begin to operate again under steady-state conditions, as shown in Figure 10a, where the COP underwent an adjustment during the operation interval, this remained around 0.7, a figure indicated for single-effect absorption refrigeration systems (Ochoa et al. 2014; Ochoa et al. 2016; Ochoa et al. 2017).

As to Figure 10b, which represents Day 2, it is important to highlight that the absorption chiller, once again, was adapted to the perturbations in the thermal load of the chilled water, and responded almost immediately, but its COP was impaired since more activation energy without obtaining more significant results in the chilled water temperature was needed, leading to values of COP around  $\pm 0.57$ , which are a little smaller than those given by the manufacturer. This phenomenon is related to the fact that the absorption refrigeration machine presents its best performance with nominal loads, namely, hot, chilled and cold temperatures of 88, 12.5 and 31°C, respectively, and mass flow rates of 2.40, 1.52 and 5.08 kg s<sup>-1</sup> of hot, chilled and cold water, respectively, which the manufacturer (Yazaki Energy System, 2003) established in accordance with the most favorable conditions of heat and mass transfer of the heat exchangers that integrated the equipment, specifically, during the desorption (generator) and absorption (absorber) process. In addition, the uncertainties of the experiments resulting from the heat fluxes were approximately  $\pm 3\%$ .

### Final considerations

It was found that the behavior of the absorption chiller had the same tendency for the two days of testing. However, the rates of heat fluxes were different, since the mass flow rates were modified, thereby changing the temperatures of the hot, chilled and cold water circuits. This is associated to the capacity of the heat exchangers because the overall coefficients and their respective flows which have been designed to dissipate heat under the maximum conditions. Another important aspect observed was the responsiveness of the system to the perturbations in the thermal load in dynamic conditions, to which the chiller adapted well, almost immediately. The system presented a lower COP when the nominal conditions were modified (at partial load), there being a decrease in the COP of 10%, but the absorption chiller responded adequately, and reduced the temperature of the chilled water.

A slight deviation between the experimentally calculated COP and those provided by the manufacturer (6%) was observed, which can be attributed to the uncertainties of the tests, and dirt in the system circuit pipes. In addition, the micro-cogeneration system was not designed to operate in experimental bench conditions, since it represents a real operation installation, where the parameters cannot be controlled as in the experiments carried out on experimental benches, where the configuration is dimensioned for this and there is no interference between the external environment and the system, in addition to which all the parameters are controlled independently, depending on the analyses performed.

Therefore, the behavior of the absorption chiller showed a strong dependence on the activation source (hot water) and the thermal load applied (chilled water), and on the cold water circuit. However, the latter is directly related to the ambient conditions, that is, humidity and air temperature, since the equipment can dissipate from these all the heat introduced by the processes of desorption and absorption.

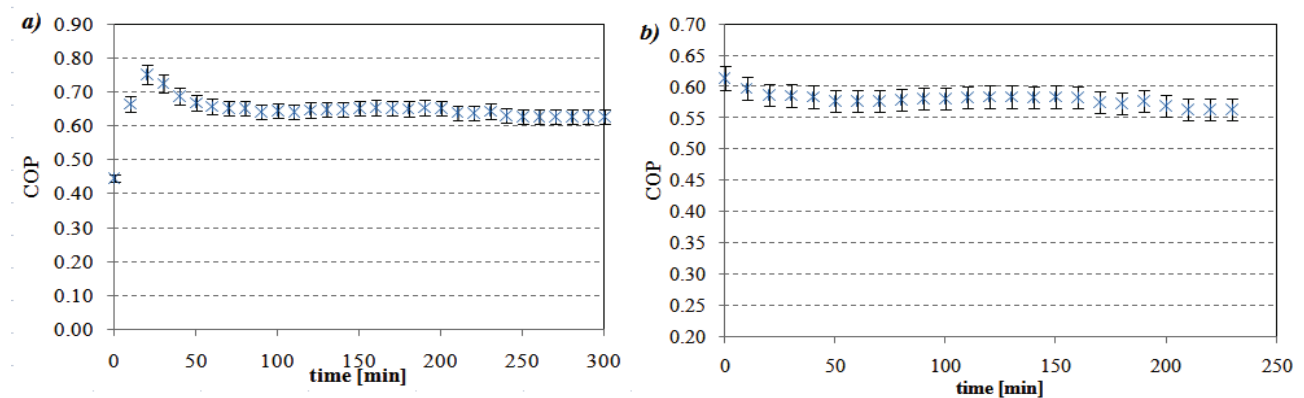


Figure 10. COP of the absorption chiller in transitory state. a) day 1. b) day 2.

### Conclusion

The performance of the dynamic absorption chiller showed positive results based on the data provided by the manufacturer, since the system responded adequately to the disturbances of the thermal load of the chilled water;

The COP value of the chiller calculated from the measured data was similar to those provided by the manufacturer under steady state conditions, with approximate values of 0.66 for Day 1 and 0.55 for Day 2.

Finally, although the absorption chiller operated at partial loads, its performance proved to be regular, but the trend of its response in transient terms was good.

### Acknowledgements

The author thanks Coordenação de Aperfeiçoamento de Pessoal de Nível Superior (Capes) for a Doctorate's degree scholarship and also the program science without border - Cnpq-Brazil, for the scholarship of the Post-doctoral study (PDE:203489/2014-4), and also the Facepe/Cnpq for financial support for research project APQ-0151-3.05/14. Moreover, the authors acknowledge Fade/Finep/Petrobrás/Copergas/UFPE for financial support of research project Proc. 21010422. The First author also thanks Professor Alberto Coronas for his support during the Post-doctoral study at the Rovira and Virgili University and also the Staff from the same university, specially the Crever group.

## References

- Edem, N. T. K., Le Pierrès, N., & Luo, L. (2012). Numerical dynamic simulation and analysis of a lithium bromide - water long-term solar heat storage system. *Energy*, *37*(1), 346-358. doi: 10.1016/j.energy.2011.11.020
- Evola, G., Le Pierrès, N., Boudehenn, F., & Papillon, P. (2013). Proposal and validation of a model for the dynamic simulation of a solar-assisted single-stage LiBr/water absorption chiller. *International Journal of Refrigeration*, *36*(3), 1015-1028. doi: 10.1016/j.ijrefrig.2012.10.013
- Gutiérrez-Urueta, G., Rodríguez, P., Ziegler, F., Lecuona, A., & Rodríguez-Hidalgo, M. C. (2012). Extension of the characteristic equation to absorption chillers with adiabatic absorbers. *International Journal of Refrigeration*, *35*(3), 709-718. doi: 10.1016/j.ijrefrig.2011.10.010
- Huicochea, A., Rivera, W., Gutiérrez, G., Bruno, J., & Coronas, A. (2011). Thermodynamic analysis of a trigeneration system consisting of a micro gas turbine and a double effect absorption chiller. *Applied Thermal Engineering*, *31*(16), 3347-3353. doi: 10.1016/j.applthermaleng.2011.06.016
- Izquierdo, M., Marcos, J. D., Palacios, M. E., & González, A. G. (2012). Experimental evaluation of a low-power direct air-cooled double-effect LiBr - H<sub>2</sub>O absorption prototype. *Energy*, *37*(1), 737-748. doi: 10.1016/j.energy.2011.10.004
- Labus, J., Bruno, J. C., & Coronas, A. (2013). Performance analysis of small capacity absorption chillers by using different modeling methods. *Applied Thermal Engineering*, *58*(1-2), 305-313. doi: 10.1016/j.applthermaleng.2013.04.032
- Marc, O., Sinama, F., Praene, J. P., Lucas, F., & Castaing-Lasvinottes, J. (2015). Dynamic modeling and experimental validation elements of a 30 kW LiBr/H<sub>2</sub>O single effect absorption chiller for solar application. *Applied Thermal Engineering*, *90*(1), 980-993. doi: 10.1016/j.applthermaleng.2015.07.067
- Monné, C., Alonso, S., Palacín, F., & Serra, F. (2011). Monitoring and simulation of an existing solar powered absorption cooling system in Zaragoza (Spain). *Applied Thermal Engineering*, *31*(1), 28-35. doi: 10.1016/j.applthermaleng.2010.08.002
- Moya, M., Bruno, J. C., Eguía, P., Torres, E., Zamora, I., & Coronas, A. (2011). Performance analysis of a trigeneration system based on a micro gas turbine and an air-cooled, indirect fired, ammonia-water absorption chiller. *Applied Energy*, *88*(12), 4424-4440. doi: 10.1016/j.apenergy.2011.05.021
- Ochoa, A. A. V., Dutra J. C. C., Henríquez, J. R. G., & Rohatgi, J. (2014). Energetic and exergetic study of a 10RT absorption chiller integrated into a microgeneration system. *Energy Conversion and Management*, *88*(1), 545-553. doi: 10.1016/j.enconman.2014.08.064
- Ochoa, A. A. V., Dutra, J. C. C., Henríquez, J. R. G., & Santos, C. A. C. (2016). Dynamic study of a single effect absorption chiller using the pair LiBr/H<sub>2</sub>O. *Energy Conversion and Management*, *108*(1), 30-42. doi: 10.1016/j.enconman.2015.11.009
- Ochoa, A. A. V., Dutra, J. C. C., Henríquez, J. R. G., Santos, C. A. C., & Rohatgi, J. (2017). The influence of the overall heat transfer coefficients in the dynamic behavior of a single effect absorption chiller using the pair LiBr/H<sub>2</sub>O. *Energy Conversion and Management*, *136*(1), 270-282. doi: 10.1016/j.enconman.2017.01.020
- Olivier, M., Praene, J., Bastide, A., & Franck, L. (2011). Modeling and experimental validation of the solar loop for absorption solar cooling system using double glazed collectors. *Applied Thermal Engineering*, *31*(2-3), 268-277. doi: 10.1016/j.applthermaleng.2010.09.006
- Ozgoren, M., Bilgili, M., & Babayigit, O. (2012). Hourly performance prediction of ammonia - water solar absorption refrigeration. *Applied Thermal Engineering*, *40*(1), 80-90. doi: 10.1016/j.applthermaleng.2012.01.058
- Popli, S., Rodgers, P., & Eveloy, V. (2013). Gas turbine efficiency enhancement using waste heat powered absorption chillers in the oil and gas industry. *Applied Thermal Engineering*, *50*(1), 918-931. doi: 10.1016/j.applthermaleng.2012.06.018
- Prasartkaew, B. (2014). Performance test of a small size LiBr-H<sub>2</sub>O absorption chiller. *Energy Procedia*, *56*(1), 487-497. doi: 10.1016/j.egypro.2014.07.183
- Puig, M., López, J., Bruno, C., & Coronas, A. (2010). Analysis and parameter identification for characteristic equations of single - and Double effect absorption chillers by means of multivariable regression. *International Journal of Refrigeration*, *33*(1), 70-78. doi: 10.1016/j.ijrefrig.2009.08.005
- Seo, J. A., Shin, Y., & Chung, J. D. (2012). Dynamics and control of solution levels in a high temperature generator for an absorption chiller. *International Journal of Refrigeration*, *35*(4), 1-7. doi: 10.1016/j.ijrefrig.2012.01.020
- Somers, C., Mortazavi, A., Hwang, Y., Radermacher, R., Rodgers, P., & Al-Hashimi, P. (2011). Modeling water/lithium bromide absorption chillers in ASPEN Plus. *Applied Energy*, *88*(11), 4197-4205. doi: 10.1016/j.apenergy.2011.05.018
- Tsoutsos, T., Aloumpi, E., Gkouskos, Z., & Karagiorgas, M. (2010). Design of a solar absorption cooling system in a Greek hospital. *Energy and Buildings*, *42*(2), 265-272. doi: 10.1016/j.enbuild.2009.09.002
- Venegas, M., Rodríguez-Hidalgo, M. C., Salgado, R., Lecuona, A., Rodríguez, P., & Gutiérrez, G. (2011). Experimental diagnosis of the influence of operational variables on the performance of a solar absorption cooling system. *Applied Energy*, *88*(4), 1447-1454. doi: 10.1016/j.apenergy.2010.10.011
- Wang, J., & Wu, J. (2015). Investigation of a mixed effect absorption chiller powered by jacket water and exhaust gas waste heat of internal combustion engine. *International Journal of Refrigeration*, *50*(1), 193-206. doi: 10.1016/j.ijrefrig.2014.11.001
- Yazaki Energy System. (2003). *Specifications chillers and chiller-heater WFC-SC (H) 10, 20, 30*. Plano, TX: Yazaki Energy System.

- Zamora, M., Bourouis, M., Coronas, A., & Vallès, M. (2014). Pre-industrial development and experimental characterization of new air-cooled and water-cooled ammonia/lithium nitrate absorption chillers. *International Journal of Refrigeration*, *45*(1), 189-197. doi: 10.1016/j.ijrefrig.2014.06.005
- Zamora, M., Bourouis, M., Coronas, A., & Vallès, M. (2015). Part-load characteristics of a new ammonia/lithium nitrate absorption chiller. *International Journal of Refrigeration*, *56*(1), 43-51. doi: 10.1016/j.ijrefrig.2014.11.005
- Zinet, M., Rulliere, R., & Haberschill, P. (2012). A numerical model for the dynamic simulation of a recirculation single-effect absorption chiller. *Energy Conversion and Management*, *62*(1), 51-63. doi: 10.1016/j.enconman.2012.04.007